

Second order numerical scheme for motion of polygonal curves with constant area speed*

Michal Beneš¹⁾, Masato Kimura²⁾ and Shigetoshi Yazaki³⁾

Abstract. We study polygonal analogues of several moving boundary problems and their time discretization which preserves the constant area speed property. We establish various polygonal analogues of geometric formulas for moving boundaries and make use of the geometric formulas for our numerical scheme and its analysis of general constant area speed motion of polygons. Accuracy and efficiency of our numerical scheme are checked through numerical simulations for several polygonal motions such as motion by curvature and area-preserving advected flow etc.

Key Words: motion of polygons, moving boundary problem, crystalline motion, crystalline curvature, motion by curvature, constant area speed motion, area-preserving numerical scheme, second order scheme

Mathematics Subject Classification (2000): 35R35, 39A12, 53C44, 65L20

1 Introduction

Polygonal analogues of several moving boundary problems and their time discretization are investigated in this paper. The polygonal motion is restricted within an equivalent class of polygons. We introduce notion of polygonal curvature, which is consistent to polygonal analogues of geometric variational formulas.

We propose a formulation of general area-preserving motion of polygonal curves by using a system of ODEs. The moving polygon belongs to a prescribed class of polygons, which is similar to the admissible class in the theory of crystalline motion by curvature. There are many articles about the crystalline curvature flow and asymptotic behavior of solutions [1, 5, 6, 8, 9, 10, 14, 15, 16, 17], etc., which started from the pioneer works [2] and [11]. Actually, if the initial curve is a convex polygon in a crystalline admissible class, then our polygonal curvature flow is nothing but the crystalline curvature flow. However, we consider more general polygonal moving boundary problems in wider admissible classes of polygons.

* The authors are supported by Czech Technical University in Prague, Faculty of Nuclear Sciences and Physical Engineering within the Jindřich Nečas Center for Mathematical Modeling (Project of the Czech Ministry of Education, Youth and Sports LC 06052).

¹⁾ Dept. of Mathematics, Faculty of Nuclear Sciences and Physical Engineering, Czech Technical University in Prague, Trojanova 13, 120 00 Prague, Czech Republic. *E-mail:* benes@kmlinux.fjfi.cvut.cz

²⁾ Faculty of Mathematics, Kyushu University, 6-10-1 Hakozaki, Fukuoka 812-8581, Japan. *E-mail:* masato@math.kyushu-u.ac.jp

³⁾ Faculty of Engineering, University of Miyazaki, 1-1 Gakuen Kibanadai Nishi, Miyazaki 889-2192, Japan. *E-mail:* yazaki@cc.miyazaki-u.ac.jp

Based on the formulation of general polygonal moving boundary problems, we propose an implicit time discretization scheme with effective iteration scheme for the nonlinear system in each time step. It has second order accuracy and preserves the constant area speed property. In a fixed admissible class of polygons, we prove a convergence theorem of second order for our numerical scheme.

On the other hand, it is expected that our polygonal analogue becomes a natural approximate solution of a smooth moving boundary problem if the number of edges is enough large. It is important and interesting application of our polygonal motion, but we do not touch on this issue in this paper. We only mention here that the crystalline algorithm and their convergence theorems for the motion by curvature are found in [5, 6, 7, 8, 11, 12, 13] etc.

The organization of this paper is as follows. Fundamental notation and formulas for polygons and polygonal motions are introduced in Section 2. In Section 3, a general initial value problem of polygonal motion in an equivalent class is considered, and the constant area speed condition is given. Several basic examples of polygonal motions such as the polygonal curvature flow and the polygonal advected flow are also presented. In Section 4, an implicit scheme of Crank-Nicolson type and an iteration scheme for the nonlinear system in each time step are proposed. The proposed scheme inherits the constant area speed property and its second order convergence is proved in Theorem 4.5. In Section 5, the accuracy of our numerical scheme is checked through various numerical simulations in comparison with the first order explicit Euler scheme. These simulation show that the second order scheme preserves the constant area speed property with high accuracy.

2 Polygons and polygonal motions

We give basic definitions and notation for the polygonal motion in an equivalent class of polygons. In particular, the polygonal curvature is introduced as a generalization of the crystalline curvature. We also collect their fundamental formulas and properties in this section.

2.1 Polygons

We define a set of polygons in \mathbb{R}^2 :

$$\mathcal{P} := \{\Gamma; \Gamma \text{ is a polygonal Jordan curve in } \mathbb{R}^2\}.$$

In this paper, we assume that any two dimensional vector $\mathbf{x} \in \mathbb{R}^2$ is represented by a column vector, and we denote its transposed row vector by \mathbf{x}^T . For $\Gamma \in \mathcal{P}$, the bounded interior polygonal domain surrounded by Γ is denoted by Ω . For simplicity, we consider

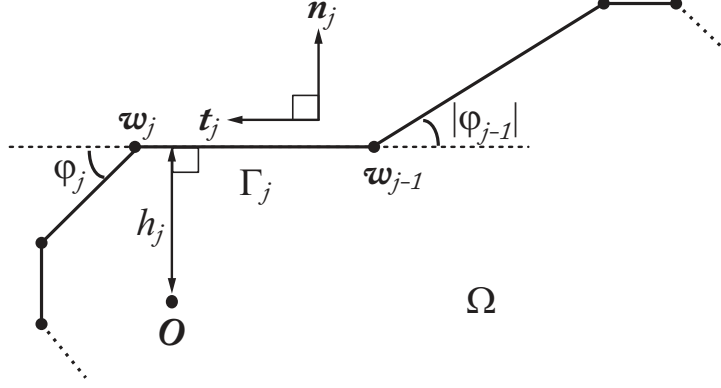


Figure 1: Some quantities defined on Γ_j .

the case that Ω is simply connected, but many of the following arguments are valid in other geometrical situations.

Let $\Gamma \in \mathcal{P}$ be an N -polygon. The N vertices of Γ are denoted by $\mathbf{w}_j \in \mathbb{R}^2$ for $j = 1, 2, \dots, N$ counterclockwise, where $\mathbf{w}_0 = \mathbf{w}_N$ and $\mathbf{w}_{N+1} = \mathbf{w}_1$. Hereafter we use the periodic numbering convention $F_0 = F_N$ and $F_{N+1} = F_1$ for any quantities defined on N -polygon.

For $j = 1, 2, \dots, N$, the j -th edge between \mathbf{w}_{j-1} and \mathbf{w}_j is defined by

$$\Gamma_j = \{(1 - \theta)\mathbf{w}_{j-1} + \theta\mathbf{w}_j; 0 < \theta < 1\},$$

and its length is denoted by $|\Gamma_j| := |\mathbf{w}_j - \mathbf{w}_{j-1}|$. The characteristic function $\chi_j \in L^\infty(\Gamma)$ for Γ_j is defined as

$$\chi_j(\mathbf{x}) := \begin{cases} 1, & \mathbf{x} \in \Gamma_j \\ 0, & \mathbf{x} \in \Gamma \setminus \Gamma_j \end{cases} \quad (j = 1, 2, \dots, N).$$

The outward unit normal on Γ_j is denoted by \mathbf{n}_j , and the outer angle at the vertex \mathbf{w}_j is denoted by $\varphi_j \in (-\pi, \pi) \setminus \{0\}$. They satisfy $\cos \varphi_j = \mathbf{n}_{j+1} \cdot \mathbf{n}_j$. We also define the height of Γ_j from the origin by $h_j := \mathbf{w}_j \cdot \mathbf{n}_j = \mathbf{w}_{j-1} \cdot \mathbf{n}_j$ (see Figure 1). Then the straight line including Γ_j is expressed by the equation $\mathbf{n}_j \cdot \mathbf{x} = h_j$, and the vertices of $\Gamma \in \mathcal{P}$ are given from $\{h_j\}_j$ as

$$\mathbf{w}_j = \begin{pmatrix} \mathbf{n}_j^T \\ \mathbf{n}_{j+1}^T \end{pmatrix}^{-1} \begin{pmatrix} h_j \\ h_{j+1} \end{pmatrix} \quad (j = 1, 2, \dots, N). \quad (2.1)$$

Proposition 2.1 *Under the above conditions, we have*

$$|\Gamma_j| = a_{j-1}h_{j-1} + b_jh_j + a_jh_{j+1} \quad (j = 1, 2, \dots, N), \quad (2.2)$$

where $a_j := \operatorname{cosec} \varphi_j$ and $b_j := -\cot \varphi_{j-1} - \cot \varphi_j$.

Proof. We define a unit tangent vector of Γ_j by $\mathbf{t}_j := (\mathbf{w}_j - \mathbf{w}_{j-1})/|\Gamma_j|$. We remark that $\mathbf{n}_{j+1} \cdot \mathbf{t}_j = -\mathbf{n}_j \cdot \mathbf{t}_{j+1} = \sin \varphi_j$ and $\mathbf{t}_j \cdot \mathbf{t}_{j+1} = \cos \varphi_j$. Then, from (2.1) and the equality:

$$\begin{pmatrix} \mathbf{n}_j^T \\ \mathbf{n}_{j+1}^T \end{pmatrix} \begin{pmatrix} -\mathbf{t}_{j+1} & \mathbf{t}_j \end{pmatrix} = \begin{pmatrix} -\mathbf{n}_j \cdot \mathbf{t}_{j+1} & 0 \\ 0 & \mathbf{n}_{j+1} \cdot \mathbf{t}_j \end{pmatrix} = \frac{1}{a_j} \begin{pmatrix} 1 & 0 \\ 0 & 1 \end{pmatrix},$$

we have

$$\mathbf{w}_j = a_j \begin{pmatrix} -\mathbf{t}_{j+1} & \mathbf{t}_j \end{pmatrix} \begin{pmatrix} h_j \\ h_{j+1} \end{pmatrix} = -\mathbf{t}_{j+1} a_j h_j + \mathbf{t}_j a_j h_{j+1}.$$

Since

$$\begin{aligned} |\Gamma_j| &= \mathbf{t}_j \cdot (\mathbf{w}_j - \mathbf{w}_{j-1}) \\ &= \mathbf{t}_j \cdot \{(-\mathbf{t}_{j+1} a_j h_j + \mathbf{t}_j a_j h_{j+1}) - (-\mathbf{t}_j a_{j-1} h_{j-1} + \mathbf{t}_{j-1} a_{j-1} h_j)\} \\ &= a_j h_{j+1} - \{a_j \cos \varphi_j + a_{j-1} \cos \varphi_{j-1}\} h_j + a_{j-1} h_{j-1} \\ &= a_j h_{j+1} + b_j h_j + a_{j-1} h_{j-1}, \end{aligned}$$

we obtain the formula (2.2). ■

The total length of Γ is given by

$$|\Gamma| := \sum_{j=1}^N |\Gamma_j| = \sum_{j=1}^N (a_j + b_j + a_{j-1}) h_j = \sum_{j=1}^N \eta_j h_j, \quad (2.3)$$

where $\eta_j := a_j + b_j + a_{j-1} = \tan(\varphi_j/2) + \tan(\varphi_{j-1}/2)$. The area of interior domain Ω is denoted by $|\Omega|$, which is given by

$$|\Omega| = \frac{1}{2} \sum_{j=1}^N |\Gamma_j| h_j. \quad (2.4)$$

The above symbols are also written as $\mathbf{n}_j = \mathbf{n}_j(\Gamma)$, $a_j = a_j(\Gamma)$ and $h_j = h_j(\Gamma)$ etc., provided we need to distinguish from quantities of the other polygons.

2.2 Equivalence classes of polygons

For two polygons Γ and $\Sigma \in \mathcal{P}$, we define an equivalence relation $\Gamma \sim \Sigma$. We say $\Gamma \sim \Sigma$, if their numbers of edges are same (let it be N) and $\mathbf{n}_j(\Gamma) = \mathbf{n}_j(\Sigma)$ for all $j = 1, 2, \dots, N$ after choosing suitable counterclockwise numbering for Γ and Σ . The equivalence class of $\Gamma \in \mathcal{P}$ is denoted by $\mathcal{P}[\Gamma] := \{\Sigma \in \mathcal{P}; \Sigma \sim \Gamma\}$.

We fix an N -polygon $\Gamma^* \in \mathcal{P}$ and let $\mathcal{P}^* := \mathcal{P}[\Gamma^*]$. For Γ and Σ in \mathcal{P}^* , we define the distance between them by

$$d(\Gamma, \Sigma) := \max_{j=1,2,\dots,N} |h_j(\Gamma) - h_j(\Sigma)|.$$

Then, it is clear that (\mathcal{P}^*, d) becomes a metric space, since it is isometrically embedded in \mathbb{R}^N equipped with maximum norm $|\cdot|_\infty$ by the height function \mathbf{h} defined on \mathcal{P}^* :

$$\mathbf{h}(\Gamma) := (h_1(\Gamma), h_2(\Gamma), \dots, h_N(\Gamma)) \in \mathbb{R}^N \quad (\Gamma \in \mathcal{P}^*).$$

We assume that vectors in \mathbb{R}^N are represented by row vectors. It is obvious that the image of the height function $\mathbf{h}(\mathcal{P}^*)$ is open in \mathbb{R}^N .

For $\Gamma \in \mathcal{P}^*$ and $\varepsilon > 0$, an ε -ball in $\mathcal{P}^* = \mathcal{P}[\Gamma]$ with center Γ is denoted by

$$B(\Gamma, \varepsilon) := \{\Sigma \in \mathcal{P}[\Gamma]; \ d(\Sigma, \Gamma) < \varepsilon\}.$$

For an open set $\mathcal{O} \subset \mathcal{P}^*$ and $\Gamma \in \mathcal{O}$, we define a positive number $\rho(\Gamma, \mathcal{O}) > 0$ as

$$\rho(\Gamma, \mathcal{O}) := \inf\{|\mathbf{a} - \mathbf{h}(\Gamma)|_\infty; \ \mathbf{a} \in \mathbb{R}^N \setminus \mathbf{h}(\mathcal{O})\}.$$

We remark that $\rho(\cdot, \mathcal{O})$ is Lipschitz continuous with Lipschitz constant 1:

$$|\rho(\Gamma, \mathcal{O}) - \rho(\Sigma, \mathcal{O})| \leq d(\Gamma, \Sigma) \quad (\Gamma, \Sigma \in \mathcal{O}).$$

For a compact set $\mathcal{K} \subset \mathcal{O}$, we also define

$$\rho(\mathcal{K}, \mathcal{O}) := \min_{\Gamma \in \mathcal{K}} \rho(\Gamma, \mathcal{O}).$$

Let $a_j = a_j(\Gamma^*)$ and $b_j = b_j(\Gamma^*)$. Then, from the formula (2.2), we obtain

$$\begin{aligned} & ||\Gamma_j| - |\Sigma_j|| \\ &= |a_{j-1}(h_{j-1}(\Gamma) - h_{j-1}(\Sigma)) + b_j(h_j(\Gamma) - h_j(\Sigma)) + a_j(h_{j+1}(\Gamma) - h_{j+1}(\Sigma))| \\ &\leq C^* d(\Gamma, \Sigma) \quad (j = 1, 2, \dots, N), \end{aligned}$$

where we define

$$C^* := \max_{l=1,2,\dots,N} \{|a_{l-1}| + |b_l| + |a_l|\}. \quad (2.5)$$

For any Γ^0 and $\Gamma^1 \in \mathcal{P}^*$ and for $\theta \in [0, 1]$, we define

$$\mathbf{h}^\theta := (1 - \theta)\mathbf{h}(\Gamma^0) + \theta\mathbf{h}(\Gamma^1) \in \mathbb{R}^N.$$

If there exists $\Gamma^\theta \in \mathcal{P}^*$ with $\mathbf{h}(\Gamma^\theta) = \mathbf{h}^\theta$, Γ^θ is called θ -interpolation of Γ^0 and Γ^1 . The θ -interpolation of $\Gamma^0 \in \mathcal{P}^*$ and $\Gamma^1 \in \mathcal{P}^*$ is denoted by $(1 - \theta)\Gamma^0 + \theta\Gamma^1 := \Gamma^\theta \in \mathcal{P}^*$.

2.3 Polygonal motions

We consider a moving polygon $\Gamma(t) \in \mathcal{P}$, where the parameter t (we call t time) belongs to an interval $\mathcal{I} \subset \mathbb{R}$. For $k \in \mathbb{N} \cup \{0\}$, we call a moving polygon $\Gamma(t)$ belongs to C^k -class on \mathcal{I} , if the number of edges of $\Gamma(t)$ does not change in time and $\mathbf{w}_j \in C^k(\mathcal{I}; \mathbb{R}^2)$ for all $j = 1, 2, \dots, N$.

If $k \geq 1$, we can define the normal velocity at $\mathbf{x} \in \Gamma_j(t)$ which is the j -th edge of $\Gamma(t)$. Let $\mathbf{n}_j(t) := \mathbf{n}_j(\Gamma(t))$. We suppose $\mathbf{x}^* \in \Gamma_j(t^*)$ and $\mathbf{x}^* = (1 - \theta)\mathbf{w}_{j-1}(t^*) + \theta\mathbf{w}_j(t^*)$ for some $\theta \in (0, 1)$, and define $\mathbf{x}(\theta, t) := (1 - \theta)\mathbf{w}_{j-1}(t) + \theta\mathbf{w}_j(t) \in \Gamma_j(t)$. Then the outward normal velocity of $\Gamma_j(t^*)$ at \mathbf{x}^* is defined by

$$V_j(\mathbf{x}^*, t^*) := \dot{\mathbf{x}}(\theta, t^*) \cdot \mathbf{n}_j(t^*) = (1 - \theta)\dot{\mathbf{w}}_{j-1}(t^*) \cdot \mathbf{n}_j(t^*) + \theta\dot{\mathbf{w}}_j(t^*) \cdot \mathbf{n}_j(t^*).$$

Here and hereafter, the (partial) derivative of \mathbf{F} with respect to t is denoted by $\dot{\mathbf{F}}$. We remark that $V_j(\cdot, t)$ is a linear function along each $\Gamma_j(t)$. We define the normal velocity of $\Gamma(t)$ by

$$V(\cdot, t) := \sum_{j=1}^N V_j(\cdot, t) \chi_j(\cdot, t) \in L^\infty(\Gamma(t)),$$

where $\chi_j(\cdot, t) \in L^\infty(\Gamma(t))$ is the characteristic function of $\Gamma_j(t)$.

If a moving polygon $\Gamma(t)$ belongs to a fixed equivalence class \mathcal{P}^* for all $t \in \mathcal{I}$, it is called *polygonal motion in \mathcal{P}^** in this paper. Let $\mathbf{h}(t) = (h_1(t), \dots, h_N(t)) \in \mathbb{R}^N$ be the height function for $\Gamma(t)$. We remark that a polygonal motion $\Gamma(t)$ in \mathcal{P}^* ($t \in \mathcal{I}$) belongs to C^k -class if and only if $\mathbf{h} \in C^k(\mathcal{I}; \mathbb{R}^N)$, from (2.1). If $\Gamma(t)$ is a C^1 -class polygonal motion in \mathcal{P}^* , its normal velocity V_j of $\Gamma_j(t)$ is a constant on each $\Gamma_j(t)$ and it is given by $V_j(t) = \dot{h}_j(t)$. We denote by $\Omega(t)$ the interior domain surrounded by $\Gamma(t)$.

Proposition 2.2 *Let $\Gamma(t)$ be a C^1 -class polygonal motion in \mathcal{P}^* . Then we have*

$$\frac{d}{dt}|\Omega(t)| = \int_{\Gamma(t)} V(\mathbf{x}, t) ds = \sum_{j=1}^N |\Gamma_j(t)| V_j(t). \quad (2.6)$$

Proof. From (2.2) and (2.4), we obtain

$$\begin{aligned} \frac{d}{dt}|\Omega(t)| &= \frac{d}{dt} \left(\frac{1}{2} \sum_{j=1}^N |\Gamma_j(t)| h_j(t) \right) \\ &= \frac{1}{2} \sum_{j=1}^N (\{a_{j-1}V_{j-1} + b_jV_j + a_jV_{j+1}\} h_j + |\Gamma_j| V_j) \\ &= \frac{1}{2} \sum_{j=1}^N V_j \{a_j h_{j+1} + b_j h_j + a_{j-1} h_{j-1}\} + \frac{1}{2} \sum_{j=1}^N |\Gamma_j| V_j \\ &= \sum_{j=1}^N |\Gamma_j| V_j. \end{aligned}$$

For $\Gamma \in \mathcal{P}^*$, the *polygonal curvature* κ_j of Γ_j is defined by

$$\kappa_j := \frac{\eta_j}{|\Gamma_j|}, \quad \eta_j := \tan \frac{\varphi_j}{2} + \tan \frac{\varphi_{j-1}}{2}.$$

We also define the polygonal curvature of Γ by

$$\kappa := \sum_{j=1}^N \kappa_j \chi_j \in L^\infty(\Gamma).$$

The reason why this is called “curvature” is shown by the following proposition.

Proposition 2.3 *Let $\Gamma(t)$ ($t \in \mathcal{I}$) be a C^1 -class polygonal motion in \mathcal{P}^* . Then*

$$\frac{d}{dt} |\Gamma(t)| = \sum_{j=1}^N |\Gamma_j(t)| \kappa_j(t) V_j(t) = \int_{\Gamma(t)} \kappa(\mathbf{x}, t) V(\mathbf{x}, t) ds.$$

Proof. We obtain

$$\frac{d}{dt} |\Gamma(t)| = \frac{d}{dt} \sum_{j=1}^N \eta_j h_j(t) = \sum_{j=1}^N \eta_j V_j(t) = \sum_{j=1}^N |\Gamma_j(t)| \kappa_j(t) V_j(t),$$

from the formula (2.3). ■

The polygonal curvature coincides with the crystalline curvature in the crystalline motion theory ([2, 11]). We, however, consider wider polygons’ classes and more general moving boundary problems. For example, we can construct a nonconvex polygon whose all edges have a constant positive polygonal curvature $\kappa_1 = \dots = \kappa_N > 0$ (see Section 5.2.4). We remark that such polygon is excluded in the standard crystalline theory.

3 Initial value problem of polygonal motion

We consider initial value problems of polygonal motions in an equivalent class. A general polygonal motion problem is formulated as a system of ODEs with respect to the height function. The notion of the constant area speed (CAS, for short) is introduced and its necessary and sufficient condition is given. Several concrete examples of the polygonal motion problems with CAS property are also presented.

3.1 General polygonal motion problem

We fix an equivalence class of N -polygons \mathcal{P}^* as in Section 2.3. For an open set $\mathcal{O} \subset \mathcal{P}^*$ and $T_* \in (0, \infty]$, let $\mathbf{F} = (F_1, \dots, F_N)$ be a given continuous function from $\mathcal{O} \times [0, T_*)$ to \mathbb{R}^N with the local Lipschitz property: For arbitrary compact set $\mathcal{K} \subset \mathcal{O}$ and $T \in (0, T_*)$, there exists $L(\mathcal{K}, T) > 0$ such that

$$|\mathbf{F}(\Gamma, t) - \mathbf{F}(\Sigma, t)|_\infty \leq L(\mathcal{K}, T) d(\Gamma, \Sigma) \quad (\Gamma, \Sigma \in \mathcal{K}, t \in [0, T]). \quad (3.1)$$

Under the condition (3.1), for a compact set $\mathcal{K} \subset \mathcal{O}$ and $T \in (0, T_*)$, we also define

$$M(\mathcal{K}, T) := \max\{|\mathbf{F}(\Gamma, t)|_\infty; \Gamma \in \mathcal{K}, t \in [0, T]\} > 0.$$

We consider the following initial value problem of polygonal motion.

Problem 3.1 *For a given N -polygon $\Gamma^* \in \mathcal{O}$, find a C^1 -class polygonal motion $\Gamma(t) \in \mathcal{O}$ ($0 \leq t \leq T < T_*$) such that*

$$\begin{cases} V_j(t) = F_j(\Gamma(t), t) & (t \in [0, T], j = 1, 2, \dots, N) \\ \Gamma(0) = \Gamma^*. \end{cases}$$

Under the Lipschitz condition (3.1), it is clear that there exists a local solution $\Gamma(t)$ in a short time interval $[0, T]$, since Problem 3.1 can be expressed by an initial value problem of an ordinary differential equations for $\mathbf{h}(t)$.

We consider the following assumption for F_j :

$$\sum_{j=1}^N |\Gamma_j| F_j(\Gamma, t) = \mu_{\text{CAS}} \quad (\Gamma \in \mathcal{O}, t \in [0, T_*)), \quad (3.2)$$

where μ_{CAS} is a fixed real number. Under the assumption (3.2), from the formula (2.6), any solution $\Gamma(t)$ to Problem 3.1 has the following property of constant area speed (CAS):

$$\frac{d}{dt} |\Omega(t)| = \mu_{\text{CAS}}.$$

3.2 Examples of problems of polygonal motion

In this section, we give some examples of polygonal motions. For several moving boundary problems for smooth curves, we can construct their polygonal analogues which naturally satisfy the basic properties such as the CAS and the curve shortening (CS, for short) properties.

Problem 3.2 (polygonal curvature flow) *For a given N -polygon $\Gamma^* \in \mathcal{P}^*$, find a C^1 -class family of N -polygons $\bigcup_{0 \leq t \leq T} \Gamma(t) \subset \mathcal{P}^*$ ($T < T_*$) satisfying*

$$\begin{cases} V_j(t) = -\kappa_j(t) & (t \in [0, T], j = 1, 2, \dots, N), \\ \Gamma(0) = \Gamma^*. \end{cases}$$

This is a polygonal analogue of the curvature flow (curve shortening problem, [4] and see references therein). In the theory of crystalline motion, Problem 3.2 is considered in a crystalline admissible class and is called the crystalline curvature motion.

Similar to the curvature flow for smooth curves, the solution of Problem 3.2 has the CS property:

$$\frac{d}{dt} |\Gamma(t)| = \sum_{j=1}^N |\Gamma_j(t)| \kappa_j(t) V_j(t) = - \sum_{j=1}^N |\Gamma_j(t)| \kappa_j(t)^2 \leq 0,$$

and the CAS property with $\mu_{\text{CAS}} = -2 \sum_{j=1}^N \tan(\varphi_j/2)$:

$$\frac{d}{dt}|\Omega(t)| = - \sum_{j=1}^N |\Gamma_j(t)|\kappa_j(t) = - \sum_{j=1}^N \eta_j = -2 \sum_{j=1}^N \tan \frac{\varphi_j}{2} = \text{const.}$$

A numerical example will be shown in Figure 2 (left).

Problem 3.3 (area-preserving polygonal curvature flow) *For a given N -polygon $\Gamma^* \in \mathcal{P}^*$, find a C^1 -class family of N -polygons $\bigcup_{0 \leq t \leq T} \Gamma(t) \subset \mathcal{P}^*$ ($T < T_*$) satisfying*

$$\begin{cases} V_j(t) = \langle \kappa(\cdot, t) \rangle - \kappa_j(t) & (t \in [0, T], j = 1, 2, \dots, N), \\ \Gamma(0) = \Gamma^*. \end{cases}$$

Here $\langle \kappa(\cdot, t) \rangle$ is the mean value of κ on $\Gamma(t)$:

$$\langle \kappa(\cdot, t) \rangle = \frac{1}{|\Gamma(t)|} \int_{\Gamma(t)} \kappa(\mathbf{x}, t) ds = \frac{\sum_{i=1}^N \eta_i}{|\Gamma(t)|} = \frac{2 \sum_{i=1}^N \tan(\varphi_i/2)}{|\Gamma(t)|}.$$

This is a polygonal analogue of the area-preserving curvature flow (see [3] etc.). Similar to the area-preserving curvature flow for smooth curves, the solution of Problem 3.3 has the CS property:

$$\frac{d}{dt}|\Gamma(t)| = \sum_{j=1}^N |\Gamma_j(t)|\kappa_j(t)V_j(t) = - \sum_{j=1}^N |\Gamma_j(t)|(\kappa_j(t) - \langle \kappa(\cdot, t) \rangle)^2 \leq 0,$$

and the CAS property with $\mu_{\text{CAS}} = 0$:

$$\frac{d}{dt}|\Omega(t)| = \langle \kappa(\cdot, t) \rangle |\Gamma(t)| - \int_{\Gamma(t)} \kappa(\mathbf{x}, t) ds = 0.$$

Some numerical examples will be shown in Figure 4.

In what follows, the mean value of \mathbf{F} on the edge Γ_j is denoted by

$$\langle \mathbf{F} \rangle_j := \frac{1}{|\Gamma_j|} \int_{\Gamma_j} \mathbf{F}(\mathbf{x}) ds.$$

Let G be a bounded Lipschitz domain in \mathbb{R}^2 . We define

$$\mathcal{O}_G := \{\Gamma \in \mathcal{P}^*; \Omega(\Gamma) \supset \overline{G}\}.$$

Problem 3.4 (polygonal advected flow with constant area speed) *Let us consider $\mathbf{u} \in C^1(\mathbb{R}^2 \setminus G; \mathbb{R}^2)$ with $\text{div } \mathbf{u} = 0$ in $\mathbb{R}^2 \setminus \overline{G}$. For a given N -polygon $\Gamma^* \in \mathcal{O}_G$, find a C^1 -class family of N -polygons $\bigcup_{0 \leq t \leq T} \Gamma(t) \subset \mathcal{O}_G$ ($T < T_*$) satisfying*

$$\begin{cases} V_j(t) = \langle \mathbf{u} \rangle_j \cdot \mathbf{n}_j & (t \in [0, T], j = 1, 2, \dots, N), \\ \Gamma(0) = \Gamma^*. \end{cases}$$

The solution has CAS property with $\mu_{\text{CAS}} = \int_{\partial G} \mathbf{n} \cdot \mathbf{u} \, ds$:

$$\begin{aligned}
\frac{d}{dt} |\Omega(t)| &= \sum_{j=1}^N |\Gamma_j(t)| \langle \mathbf{u} \rangle_j \cdot \mathbf{n}_j \\
&= \sum_{j=1}^N \int_{\Gamma_j(t)} \mathbf{u} \cdot \mathbf{n}_j \, ds \\
&= \int_{\partial G} \mathbf{u} \cdot \mathbf{n} \, ds - \int_{\Omega(t) \setminus \bar{G}} \operatorname{div} \mathbf{u} \, d\mathbf{x} \\
&= \int_{\partial G} \mathbf{u} \cdot \mathbf{n} \, ds,
\end{aligned}$$

where \mathbf{n} is the unit normal vector on ∂G pointing to interior of G . A numerical example will be shown in Figure 6.

4 Numerical schemes

In this section, we propose an implicit time discretization of Crank-Nicolson type to solve the general initial value problem of polygonal motions (Problem 3.1) and show that it preserves the CAS property and has a second order accuracy. We also propose an effective iteration scheme to solve a nonlinear system which appears in each time step. For comparisons, we also consider an explicit Euler scheme. We additionally give comments on the curve shortening and constant length speed properties and their numerical preservation.

4.1 Notation

In Section 4, we consider time discretization of Problem 3.1 with the following notation. The discrete time steps are denoted by $0 = t_0 < t_1 < t_2 < \dots < t_{\bar{m}} \leq T$. The step size which may be nonuniform and their maximum size are defined by

$$\tau_m := t_{m+1} - t_m \quad (m = 0, 1, \dots, \bar{m} - 1), \quad \tau := \max_{0 \leq m < \bar{m}} \tau_m.$$

Approximate solution of $\Gamma(t_m)$ is denoted by $\Gamma^m \in \mathcal{P}^*$. Quantities of the polygon Γ^m are denoted by $\mathbf{h}^m = (h_1^m, \dots, h_N^m) := (h_1(\Gamma^m), \dots, h_N(\Gamma^m))$, and $\kappa_j^m := \kappa_j(\Gamma^m)$, etc. We define $\mathbf{e}^m := \mathbf{h}(t_m) - \mathbf{h}^m \in \mathbb{R}^N$. Then we have $d(\Gamma(t_m), \Gamma^m) = |\mathbf{e}^m|_\infty$.

The discrete normal velocity $\mathbf{V}^m = (V_1^m, \dots, V_N^m)$, which is an approximation of $\mathbf{V}(t_m) = \dot{\mathbf{h}}(t_m)$, is defined by

$$\mathbf{V}^m := \frac{\mathbf{h}^{m+1} - \mathbf{h}^m}{\tau_m} \quad (m = 0, 1, \dots, \bar{m} - 1). \quad (4.1)$$

Corresponding to the formula (2.6), the following formula holds.

$$\frac{|\Omega^{m+1}| - |\Omega^m|}{\tau_m} = \sum_{j=1}^N \frac{|\Gamma_j^m| + |\Gamma_j^{m+1}|}{2} V_j^m. \quad (4.2)$$

This has a form of sum of areas of N trapezoids and is derived from (2.4) as follows:

$$\begin{aligned}
|\Omega^{m+1}| - |\Omega^m| &= \frac{1}{2} \sum_{j=1}^N (|\Gamma_j^{m+1}| h_j^{m+1} - |\Gamma_j^m| h_j^m) \\
&= \frac{1}{2} \sum_{j=1}^N \{ (|\Gamma_j^{m+1}| + |\Gamma_j^m|) (h_j^{m+1} - h_j^m) + |\Gamma_j^{m+1}| h_j^m - |\Gamma_j^m| h_j^{m+1} \} \\
&= \frac{\tau_m}{2} \sum_{j=1}^N (|\Gamma_j^{m+1}| + |\Gamma_j^m|) V_j^m + \frac{1}{2} \sum_{j=1}^N (|\Gamma_j^{m+1}| h_j^m - |\Gamma_j^m| h_j^{m+1}),
\end{aligned}$$

where the last sum is equal to zero due to the equality (2.2).

In the following sections, we suppose that there exists a unique solution $\Gamma(t)$ for $0 \leq t \leq T < T_*$ to Problem 3.1 under the condition (3.1), and that discrete time steps $0 = t_0 < t_1 < t_2 < \dots < t_{\bar{m}} \leq T$ are given a priori such as the uniform time stepping $t_m = m\tau$. We adopt the uniform time increment in the numerical examples in Section 5. It is, however, possible to apply any a posteriori adaptive time step control scheme. Similar to the finite time extinction of the curvature flow of smooth curves, even in the polygonal motions, the solution polygon often has singularities in finite time. For instance, $|\Gamma_j(t)|$ tends to zero, in other words, $|\kappa_j(t)|$ tends to infinity. A posteriori adaptive time step control will be required near the blow-up time for accurate computation.

4.2 Second order implicit scheme

We consider the following implicit scheme for Problem 3.1.

Problem 4.1 *For a given N -polygon $\Gamma_* \in \mathcal{O}$ and given time steps $0 = t_0 < t_1 < t_2 < \dots < t_{\bar{m}} \leq T$, find polygons $\Gamma^m \in \mathcal{O}$ ($m = 1, 2, \dots, \bar{m}$) such that*

$$\begin{cases} V_j^m = F_j(\Gamma^{m+1/2}, t_{m+1/2}) & (m = 0, 1, 2, \dots, \bar{m} - 1, j = 1, 2, \dots, N), \\ \Gamma^0 = \Gamma_*, \end{cases}$$

where $\Gamma^{m+1/2}$ and $t_{m+1/2}$ are the 1/2-interpolations:

$$\Gamma^{m+1/2} := \frac{\Gamma^m + \Gamma^{m+1}}{2} \in \mathcal{P}^*, \quad t_{m+1/2} := \frac{t_m + t_{m+1}}{2} = t_m + \frac{\tau_m}{2}.$$

This is a generalized version of the scheme presented in [13] for area-preserving crystalline curvature flow.

Theorem 4.2 *We suppose the CAS property (3.2). Let $\Gamma^m \in \mathcal{O}$ ($m = 1, 2, \dots, \bar{m}$) be a solution of Problem 4.1. Then it satisfies*

$$|\Omega^{m+1}| = |\Omega^m| + \mu_{CAS} \tau_m \quad (m = 0, 1, \dots, \bar{m} - 1).$$

In other words, $|\Omega^m| = |\Omega(t_m)|$ holds if the exact solution $\Omega(t)$ of Problem 3.1 exists.

Proof. Since $|\Gamma_j^{m+1/2}| = (|\Gamma_j^m| + |\Gamma_j^{m+1}|)/2$, we have

$$\frac{|\Omega^{m+1}| - |\Omega^m|}{\tau_m} = \sum_{j=1}^N |\Gamma_j^{m+1/2}| F_j(\Gamma^{m+1/2}, t_{m+1/2}) = \mu_{\text{CAS}},$$

from the formula (4.2). ■

We remark that the numerical scheme Problem 4.1 inherits the CAS property but does not depend on the area speed μ_{CAS} .

Since Problem 4.1 is an implicit scheme, it is not clear whether $\Gamma^{m+1} \in \mathcal{O}$ can be determined uniquely from the previous polygon $\Gamma^m \in \mathcal{O}$, the time t_m , and the time step size τ_m . Another question is how to solve the equations

$$\mathbf{h}^{m+1} = \mathbf{h}^m + \tau_m \mathbf{F} \left(\frac{\Gamma^m + \Gamma^{m+1}}{2}, t_{m+1/2} \right), \quad (4.3)$$

to obtain (approximation of) Γ^{m+1} numerically. The answers to these questions will be given in Theorem 4.4 and 4.5.

We fix $\hat{\Gamma} \in \mathcal{O}$ and $\hat{t} \in [0, T]$, which correspond to Γ^m and $t_{m+1/2}$, respectively. Let \mathcal{K} be a compact convex set in \mathcal{P}^* with $\hat{\Gamma} \in \mathcal{K} \subset \mathcal{O}$. For $\Sigma \in \mathcal{K}$ and $\hat{\tau} \in (0, \rho(\hat{\Gamma}, \mathcal{O})M(\mathcal{K}, T)^{-1})$, we can define $\tilde{\Sigma} \in \mathcal{O}$ by

$$\mathbf{h}(\tilde{\Sigma}) = \mathbf{h}(\hat{\Gamma}) + \hat{\tau} \mathbf{F} \left(\frac{\hat{\Gamma} + \Sigma}{2}, \hat{t} \right).$$

We define $\Lambda(\Sigma) := \Lambda(\Sigma; \hat{\Gamma}, \hat{t}, \hat{\tau}) := \tilde{\Sigma}$. Then Λ becomes a mapping from \mathcal{K} to \mathcal{O} . We have the following lemma.

Lemma 4.3 *Let $\varepsilon \in (0, \rho(\hat{\Gamma}, \mathcal{O}))$ and $\lambda \in (0, 1)$ be fixed, and let $\hat{\mathcal{K}} := \overline{B(\hat{\Gamma}, \varepsilon)}$. Suppose that $\hat{\tau}$ satisfies the condition:*

$$0 < \hat{\tau} \leq \min \left\{ T - \hat{t}, \frac{\varepsilon}{M(\hat{\mathcal{K}}, T)}, \frac{2\lambda}{L(\hat{\mathcal{K}}, T)} \right\}.$$

Then Λ maps $\hat{\mathcal{K}}$ into $\hat{\mathcal{K}}$ and satisfies

$$d(\Lambda(\Sigma^1), \Lambda(\Sigma^2)) \leq \lambda d(\Sigma^1, \Sigma^2) \quad (\Sigma^1, \Sigma^2 \in \hat{\mathcal{K}}). \quad (4.4)$$

Namely, Λ is a contraction mapping on $\hat{\mathcal{K}}$ and there exists a unique fixed point of Λ in $\hat{\mathcal{K}}$.

Proof. Let $\Sigma \in \hat{\mathcal{K}}$. Since $\hat{\mathcal{K}}$ is convex, $(\hat{\Gamma} + \Sigma)/2 \in \hat{\mathcal{K}}$ holds. We also have

$$\left| \mathbf{h}(\tilde{\Sigma}) - \mathbf{h}(\hat{\Gamma}) \right|_{\infty} = \left| \hat{\tau} \mathbf{F} \left(\frac{\hat{\Gamma} + \Sigma}{2}, \hat{t} \right) \right|_{\infty} \leq \hat{\tau} M(\hat{\mathcal{K}}, T) \leq \varepsilon.$$

This estimate shows that Λ is a mapping from $\hat{\mathcal{K}}$ into itself. The estimate (4.4) is proved as follows:

$$\begin{aligned}
& d(\Lambda(\Sigma^1), \Lambda(\Sigma^2)) \\
&= |\mathbf{h}(\Lambda(\Sigma^1)) - \mathbf{h}(\Lambda(\Sigma^2))|_\infty = \hat{\tau} \left| \mathbf{F} \left(\frac{\hat{\Gamma} + \Sigma^1}{2}, \hat{t} \right) - \mathbf{F} \left(\frac{\hat{\Gamma} + \Sigma^2}{2}, \hat{t} \right) \right|_\infty \\
&\leq \hat{\tau} L(\hat{\mathcal{K}}, T) d \left(\frac{\hat{\Gamma} + \Sigma^1}{2}, \frac{\hat{\Gamma} + \Sigma^2}{2} \right) \\
&= \hat{\tau} L(\hat{\mathcal{K}}, T) \left| \frac{\mathbf{h}(\hat{\Gamma}) + \mathbf{h}(\Sigma^1)}{2} - \frac{\mathbf{h}(\hat{\Gamma}) + \mathbf{h}(\Sigma^2)}{2} \right|_\infty \\
&= \frac{\hat{\tau}}{2} L(\hat{\mathcal{K}}, T) d(\Sigma^1, \Sigma^2) \leq \lambda d(\Sigma^1, \Sigma^2).
\end{aligned}$$

■

The following theorem gives us an efficient numerical scheme to obtain Γ^{m+1} . The proof is clear from Lemma 4.3.

Theorem 4.4 *Let \mathcal{K} be a compact set in \mathcal{O} and let $\varepsilon \in (0, \rho(\mathcal{K}, \mathcal{O}))$. We define*

$$\mathcal{K}_\varepsilon := \overline{\bigcup_{\Sigma \in \mathcal{K}} B(\Sigma, \varepsilon)}.$$

For fixed m ($< \bar{m}$) in Problem 4.1, we assume that $\Gamma^m \in \mathcal{K}$ and

$$\tau_m \leq \min \left\{ \frac{\varepsilon}{M(\mathcal{K}_\varepsilon, T)}, \frac{2\lambda}{L(\mathcal{K}_\varepsilon, T)} \right\},$$

where $\lambda \in (0, 1)$. Then there exists uniquely $\Gamma^{m+1} \in \overline{B(\Gamma^m, \varepsilon)}$ satisfying (4.3).

Furthermore, Γ^{m+1} is a fixed point of the contraction $\Lambda_m := \Lambda(\cdot; \Gamma^m, t_m, \tau_m)$ in $\overline{B(\Gamma^m, \varepsilon)}$, and is given by the limit of $\Lambda_m^\nu(\Gamma^m)$ as $\nu \rightarrow \infty$ with the following estimate

$$d(\Gamma^{m+1}, \Lambda_m^\nu(\Gamma^m)) \leq \lambda^\nu d(\Gamma^{m+1}, \Gamma^m) \quad (\nu \in \mathbb{N}).$$

From this theorem, $\Lambda_m^\nu(\Gamma^m)$ for sufficiently large ν gives a satisfactory approximation of Γ^{m+1} . An iteration algorithm based on this idea will be given in Section 5.1. The following theorem shows the second order convergence of the implicit numerical scheme (Problem 4.1).

Theorem 4.5 *We suppose that $\{\Gamma(t)\}_{0 \leq t \leq T}$ be a C^{k+1} -class solution of Problem 3.1 for $k = 0, 1$, or 2 . There exists $\delta^* > 0$, $\tau^* > 0$, $C > 0$ and a non-decreasing function $\omega(a) > 0$ with*

$$\omega(a) = \begin{cases} o(a^k) & \text{if } k = 0 \text{ or } 1, \\ O(a^2) & \text{if } k = 2, \end{cases} \quad \text{as } a \downarrow 0, \quad (4.5)$$

such that, if $d(\Gamma^*, \Gamma^0) \leq \delta^*$ and $\tau \leq \tau^*$, then $\Gamma^m \in \mathcal{O}$ ($m = 1, 2, \dots, \bar{m}$) are inductively determined by the implicit scheme (Problem 4.1) and

$$\max_{0 \leq m \leq \bar{m}} d(\Gamma(t_m), \Gamma^m) \leq \omega(\tau) + Cd(\Gamma(0), \Gamma^0),$$

holds.

Proof. We put $\hat{\rho} := \rho(\{\Gamma(t); 0 \leq t \leq T\}, \mathcal{O})$, and fix $\delta \in (0, \hat{\rho})$ and $\varepsilon \in (0, \hat{\rho} - \delta)$. We define

$$\begin{aligned} \mathcal{K} &:= \overline{\bigcup_{0 \leq t \leq T} B(\Gamma(t), \delta)}, \quad \mathcal{K}_\varepsilon := \overline{\bigcup_{\Sigma \in \mathcal{K}} B(\Sigma, \varepsilon)}, \\ L &:= L(\mathcal{K}_\varepsilon, T), \quad R(a) := e^{\frac{L}{2}} \left(1 - \frac{aL}{2}\right)^{-1/a} \quad (0 < a < 2/L), \\ p_m &:= |e^m|_\infty + \frac{\omega(\tau)}{L} \quad (m = 0, 1, 2, \dots, \bar{m}), \end{aligned}$$

where a non-decreasing function $\omega(a)$ ($0 < a < T$), which satisfies (4.5), will be defined in (4.9) later. Since $R(\cdot)$ is an increasing function, there exists $\delta^* > 0$ and $\tau^* > 0$ such that

$$R(\tau^*)^T \left(\delta^* + \frac{\omega(\tau^*)}{L} \right) \leq \delta, \quad \tau^* < \min \left(\frac{\varepsilon}{M(\mathcal{K}_\varepsilon, T)}, \frac{2}{L} \right).$$

For $m = 0, 1, 2, \dots, \bar{m} - 1$, we will prove the following inductive conditions:

$$\Gamma^m \in \mathcal{K}, \quad p_m \leq R(\tau)^{t_m} p_0 \quad \Rightarrow \quad \exists \Gamma^{m+1} \in \mathcal{K}, \quad p_{m+1} \leq R(\tau)^{t_{m+1}} p_0. \quad (4.6)$$

The conditions $\Gamma^0 \in \mathcal{K}$ and $p_0 \leq R(\tau)^0 p_0$ for the case $m = 0$ are obviously satisfied.

Let us assume the conditions $\Gamma^m \in \mathcal{K}$ and $p_m \leq R(\tau)^{t_m} p_0$ for a fixed m . Then, from Theorem 4.4, there exists Γ^{m+1} uniquely in $\overline{B(\Gamma^m, \varepsilon)} \subset \mathcal{K}_\varepsilon$, and we have

$$e^{m+1} - e^m = \mathbf{h}(t_{m+1}) - \mathbf{h}(t_m) - \tau_m \mathbf{V}^m = \tau_m \left\{ \boldsymbol{\xi}^m + (\mathbf{V}(t_{m+1/2}) - \mathbf{V}^m) \right\}, \quad (4.7)$$

$$\boldsymbol{\xi}^m := \frac{\mathbf{h}(t_{m+1}) - \mathbf{h}(t_m)}{\tau_m} - \dot{\mathbf{h}}(t_{m+1/2}).$$

The last term of (4.7) is estimated as follows. Since $\Gamma(t_{m+1/2}) \in \mathcal{K} \subset \mathcal{K}_\varepsilon$ and $\Gamma^{m+1/2} \in \overline{B(\Gamma^m, \varepsilon)} \subset \mathcal{K}_\varepsilon$, we have

$$\begin{aligned} & \|\mathbf{V}(t_{m+1/2}) - \mathbf{V}^m\|_\infty \\ &= \|\mathbf{F}(\Gamma(t_{m+1/2}), t_{m+1/2}) - \mathbf{F}(\Gamma^{m+1/2}, t_{m+1/2})\|_\infty \leq Ld(\Gamma(t_{m+1/2}), \Gamma^{m+1/2}) \\ &= L \left\| \mathbf{h}(t_{m+1/2}) - \frac{\mathbf{h}^m + \mathbf{h}^{m+1}}{2} \right\|_\infty = L \left\| \frac{1}{2}(e^m + e^{m+1}) - \boldsymbol{\xi}^m \right\|_\infty, \end{aligned} \quad (4.8)$$

where

$$\boldsymbol{\zeta}^m := \frac{\mathbf{h}(t_m) + \mathbf{h}(t_{m+1})}{2} - \mathbf{h}(t_{m+1/2}).$$

Combining (4.7) and (4.8), we obtain

$$\begin{aligned} |\mathbf{e}^{m+1}|_\infty &\leq |\mathbf{e}^m|_\infty + \tau_m |\boldsymbol{\xi}^m|_\infty + \tau_m L \left| \frac{1}{2}(\mathbf{e}^m + \mathbf{e}^{m+1}) - \boldsymbol{\zeta}^m \right|_\infty \\ &\leq |\mathbf{e}^m|_\infty + \frac{\tau_m L}{2} (|\mathbf{e}^{m+1}|_\infty + |\mathbf{e}^m|_\infty) + \tau_m (|\boldsymbol{\xi}^m|_\infty + L|\boldsymbol{\zeta}^m|_\infty). \end{aligned}$$

By the Taylor expansion, we can obtain an non-decreasing function $\omega(a)$ ($0 < a < T$) which satisfies the condition (4.5) and the inequality

$$|\boldsymbol{\xi}^m|_\infty + L|\boldsymbol{\zeta}^m|_\infty \leq \omega(\tau). \quad (4.9)$$

Hence, we have

$$\left(1 - \frac{\tau_m L}{2}\right) |\mathbf{e}^{m+1}|_\infty \leq \left(1 + \frac{\tau_m L}{2}\right) |\mathbf{e}^m|_\infty + \tau_m \omega(\tau),$$

and this inequality is equivalent to

$$\left(1 - \frac{\tau_m L}{2}\right) p_{m+1} \leq \left(1 + \frac{\tau_m L}{2}\right) p_m.$$

From the inequalities

$$\left(1 - \frac{\tau_m L}{2}\right) \geq \left(1 - \frac{\tau L}{2}\right)^{\tau_m/\tau} \quad \text{and} \quad \left(1 + \frac{\tau_m L}{2}\right) \leq e^{\tau_m L/2},$$

we obtain

$$p_{m+1} \leq \left(1 - \frac{\tau_m L}{2}\right)^{-1} \left(1 + \frac{\tau_m L}{2}\right) p_m \leq R(\tau)^{\tau_m} (R(\tau)^{t_m} p_0) \leq R(\tau)^{t_{m+1}} p_0.$$

The condition $\Gamma^{m+1} \in \mathcal{K}$ follows from this estimate as

$$|\mathbf{e}^{m+1}|_\infty \leq p_{m+1} \leq R(\tau^*)^{t_{m+1}} p_0 \leq R(\tau^*)^T \left(\delta^* + \frac{\omega(\tau^*)}{L} \right) \leq \delta.$$

Hence, we have proved (4.6), which leads us to the estimate:

$$|\mathbf{e}^m|_\infty \leq R(\tau^*)^T \left(|\mathbf{e}^0|_\infty + \frac{\omega(\tau)}{L} \right) - \frac{\omega(\tau)}{L} \leq R(\tau^*)^T |\mathbf{e}^0|_\infty + \frac{R(\tau^*)^T - 1}{L} \omega(\tau).$$

The assertion of the theorem is obtained by putting $C := R(\tau^*)^T$ and denoting the last term $L^{-1}(R(\tau^*)^T - 1)\omega(\tau)$ again by $\omega(\tau)$. ■

4.3 Euler scheme

For Problem 3.1, one of the simplest numerical scheme is the following explicit Euler scheme:

Problem 4.6 *For a given N -polygon $\Gamma_* \in \mathcal{O}$ and time steps $0 = t_0 < t_1 < t_2 < \dots < t_{\bar{m}} \leq T$, find polygons $\Gamma^m \in \mathcal{O}$ ($m = 1, 2, \dots, \bar{m}$) such that*

$$\begin{cases} V_j^m = F_j(\Gamma^m, t_m) & (m = 0, 1, 2, \dots, \bar{m} - 1, j = 1, 2, \dots, N), \\ \Gamma^0 = \Gamma_*. \end{cases}$$

The explicit Euler scheme is simple but it has only first order accuracy. In particular, for polygonal motions with CAS property, we are required to use a more accurate scheme such as Problem 4.1 in order to keep its CAS property numerically. Similarly to the case of the implicit scheme (Theorem 4.5), the convergence theorem of the Euler scheme is stated as follows.

Theorem 4.7 *We suppose the condition (3.1) and that $\{\Gamma(t)\}_{0 \leq t \leq T}$ be a C^{k+1} -class solution of Problem 3.1 for $k = 0$ or 1 . There exists $\delta^* > 0$, $\tau^* > 0$, $C > 0$ and a non-decreasing function $\omega(a) > 0$ with*

$$\omega(a) = \begin{cases} o(1) & \text{if } k = 0, \\ O(a) & \text{if } k = 1, \end{cases} \quad \text{as } a \downarrow 0, \quad (4.10)$$

such that, if $d(\Gamma^, \Gamma^0) \leq \delta^*$ and $\tau \leq \tau^*$, then $\Gamma^m \in \mathcal{O}$ ($m = 1, 2, \dots, \bar{m}$) is determined by the Euler scheme (Problem 4.6) and satisfies the estimate*

$$\max_{0 \leq m \leq \bar{m}} d(\Gamma(t_m), \Gamma^m) \leq \omega(\tau) + Cd(\Gamma(0), \Gamma^0).$$

Proof. We define

$$\xi^m := \frac{\mathbf{h}(t_{m+1}) - \mathbf{h}(t_m)}{\tau_m} - \dot{\mathbf{h}}(t_m) \quad (m = 0, \dots, \bar{m} - 1).$$

Then, by the Taylor expansion, we are able to find an non-decreasing function $\omega(a)$ ($0 < a < T$) which satisfies the condition (4.10) and the inequality

$$|\xi^m|_\infty \leq \omega(\tau). \quad (4.11)$$

We put $\hat{\rho} := \rho(\{\Gamma(t); 0 \leq t \leq T\}, \mathcal{O})$, and fix $\delta \in (0, \hat{\rho})$ and $\varepsilon \in (0, \hat{\rho} - \delta)$. We define

$$\begin{aligned} \mathcal{K} &:= \overline{\bigcup_{0 \leq t \leq T} B(\Gamma(t), \delta)}, \quad \mathcal{K}_\varepsilon := \overline{\bigcup_{\Sigma \in \mathcal{K}} B(\Sigma, \varepsilon)}, \\ L &:= L(\mathcal{K}, T), \quad p_m := |e^m|_\infty + \frac{\omega(\tau)}{L} \quad (m = 0, 1, 2, \dots, \bar{m}). \end{aligned}$$

There exists $\delta^* > 0$ and $\tau^* > 0$ such that

$$e^{TL} \left(\delta^* + \frac{\omega(\tau^*)}{L} \right) \leq \delta, \quad \tau^* \leq \frac{\varepsilon}{M(\mathcal{K}, T)}.$$

For $m = 0, 1, 2, \dots, \bar{m} - 1$, we will prove the following inductive conditions:

$$\Gamma^m \in \mathcal{K}, \quad p_m \leq e^{t_m L} p_0 \quad \Rightarrow \quad \exists \Gamma^{m+1} \in \mathcal{K}, \quad p_{m+1} \leq e^{t_{m+1} L} p_0. \quad (4.12)$$

The condition for $m = 0$ are obviously satisfied.

Let us assume the conditions $\Gamma^m \in \mathcal{K}$ and $p_m \leq e^{t_m L} p_0$ for a fixed m . Then, from the condition $\tau^* \leq \varepsilon/M(\mathcal{K}, T)$, Γ^{m+1} belongs to $\overline{B(\Gamma^m, \varepsilon)} \subset \mathcal{K}_\varepsilon$, and we have

$$\mathbf{e}^{m+1} - \mathbf{e}^m = \mathbf{h}(t_{m+1}) - \mathbf{h}(t_m) - \tau_m \mathbf{V}^m = \tau_m \{ \boldsymbol{\xi}^m + (\mathbf{V}(t_m) - \mathbf{V}^m) \}. \quad (4.13)$$

Since $\Gamma(t_m)$ and Γ^m both belong to \mathcal{K} , we have

$$|\mathbf{V}(t_m) - \mathbf{V}^m|_\infty = |\mathbf{F}(\Gamma(t_m), t_m) - \mathbf{F}(\Gamma^m, t_m)|_\infty \leq L d(\Gamma(t_m), \Gamma^m) = L |\mathbf{e}^m|_\infty. \quad (4.14)$$

Combining (4.11), (4.13) and (4.14), we obtain

$$|\mathbf{e}^{m+1}|_\infty \leq (1 + \tau_m L) |\mathbf{e}^m|_\infty + \tau_m \omega(\tau),$$

and

$$p_{m+1} \leq (1 + \tau_m L) p_m \leq e^{\tau_m L} (e^{t_m L} p_0) = e^{t_{m+1} L} p_0.$$

Since

$$|\mathbf{e}^{m+1}|_\infty \leq p_{m+1} \leq e^{t_{m+1} L} p_0 \leq e^{TL} \left(\delta^* + \frac{\omega(\tau^*)}{L} \right) \leq \delta,$$

the condition $\Gamma^{m+1} \in \mathcal{K}$ follows. Hence, we have proved (4.12), which leads us to the estimate:

$$|\mathbf{e}^m|_\infty \leq e^{LT} \left(|\mathbf{e}^0|_\infty + \frac{\omega(\tau)}{L} \right) - \frac{\omega(\tau)}{L} \leq e^{LT} |\mathbf{e}^0|_\infty + \frac{e^{LT} - 1}{L} \omega(\tau).$$

The assertion of the theorem is obtained by putting $C := e^{LT}$ and denoting the last term $L^{-1}(e^{LT} - 1)\omega(\tau)$ again by $\omega(\tau)$. ■

4.4 Curve shortening and constant length speed property

As seen in Section 3.2, many moving boundary problems hold the CS property:

$$\frac{d}{dt} |\Gamma(t)| \leq 0.$$

From (2.3), a necessary and sufficient condition for CS property is

$$\sum_{j=1}^N \eta_j F_j(\Gamma, t) \leq 0 \quad (\Gamma \in \mathcal{O}, \quad t \in [0, T_*]). \quad (4.15)$$

Similarly to the CAS property (3.2), we can also consider constant length speed (CLS, for short) property:

$$\frac{d}{dt} |\Gamma(t)| = \mu_{\text{CLS}}.$$

A necessary and sufficient condition for CLS property is

$$\sum_{j=1}^N \eta_j F_j(\Gamma, t) = \mu_{\text{CLS}} \quad (\Gamma \in \mathcal{O}, t \in [0, T_*)). \quad (4.16)$$

An example with CLS property is the constant speed motion:

$$F_j(\Gamma, t) = 1 \quad (j = 1, \dots, N), \quad \mu_{\text{CLS}} = 2 \sum_{j=1}^N \tan \frac{\varphi_j}{2}.$$

Another example is the length-preserving polygonal curvature flow:

$$F_j(\Gamma, t) = \frac{\sum_{i=1}^N |\Gamma_j| \kappa_j(\Gamma)^2}{2 \sum_{i=1}^N \tan(\varphi_i/2)} - \kappa_j(\Gamma) \quad (j = 1, \dots, N), \quad \mu_{\text{CLS}} = 0. \quad (4.17)$$

It is easy to check that both the second order implicit scheme (Problem 4.1) and the explicit Euler scheme (Problem 4.3) inherit the CS and CLS properties. Namely, under the condition (4.15), we have

$$|\Gamma^{m+1}| \leq |\Gamma^m| \quad (m = 0, 1, \dots, \bar{m} - 1),$$

and, under the condition (4.16), we have

$$|\Gamma^{m+1}| = |\Gamma^m| + \mu_{\text{CLS}} \tau_m \quad (m = 0, 1, \dots, \bar{m} - 1).$$

A numerical simulation for the length-preserving polygonal curvature flow will be shown in Figure 8.

5 Numerical computation

We describe an algorithm of our second order implicit scheme and show some numerical results. In this section, $\Gamma^m \in \mathcal{P}^*$ ($m = 0, 1, \dots, \bar{m}$) denotes the numerical solution computed by the algorithm described in Section 5.1. All computations are performed in double precision.

5.1 Algorithm

We describe a numerical procedure of Problem 4.1. We suppose that an initial N -polygon $\Gamma^0 = \bigcup_{j=1}^N \overline{\Gamma_j^0}$ is given in a prescribed equivalence class \mathcal{P}^* , i.e., $\mathcal{P}^* = \mathcal{P}[\Gamma^0]$. In other words, the set of normal vectors $\{\mathbf{n}_j\}_{j=1}^N$ for \mathcal{P}^* and the set of heights of Γ_j^0 $\mathbf{h}^0 = (h_1^0, \dots, h_N^0) \in \mathbb{R}^N$ are given. The outer angles $\{\varphi_j\}_{j=1}^N$ and the quantities $\{a_j\}_{j=1}^N$, $\{b_j\}_{j=1}^N$ are computed from $\{\mathbf{n}_j\}_{j=1}^N$. We fix the maximum computation time T_* and the uniform time step $\tau = T_*/\bar{m}$ with the maximum time step \bar{m} .

Then $\Gamma^{m+1} \in \mathcal{P}^*$ is determined successively from $\Gamma^m \in \mathcal{P}^*$ at the m -th discrete time $t_m = m\tau$ for $m = 0, 1, \dots, \bar{m} - 1$ as follows. We suppose the set of heights of

$\Gamma_j^m \mathbf{h}^m = (h_1^m, \dots, h_N^m) \in \mathbb{R}^N$ are given. We can calculate the j -th vertex \mathbf{w}_j^m of Γ^m by (2.1) ($j = 1, 2, \dots, N$). Our algorithm including the iteration scheme to obtain an approximation of Γ^{m+1} is as follows.

- (1) Put $\bar{\mathbf{h}} := \mathbf{h}^m$.
- (2) Define $\hat{\Gamma} \in \mathcal{P}^*$ with $\mathbf{h}(\hat{\Gamma}) = \bar{\mathbf{h}}$ and put $\hat{\mathbf{h}} := \bar{\mathbf{h}}$.
- (3) Compute $\bar{\mathbf{h}} := \mathbf{h}^m + \mathbf{F}(\hat{\Gamma}, t_{m+1/2}) \tau/2$.
- (4) If $|\bar{\mathbf{h}} - \hat{\mathbf{h}}|_\infty \leq \varepsilon/2$, then go to step (6).
- (5) Go to step (2).
- (6) Put $\mathbf{h}^{m+1} := 2\bar{\mathbf{h}} - \mathbf{h}^m$.

We note that $\hat{\Gamma}$ and $\bar{\Gamma}$ (with $\mathbf{h}(\bar{\Gamma}) = \bar{\mathbf{h}}$) in step (3) correspond to $(\Lambda_m^\nu(\Gamma^m) + \Gamma^m)/2$ and $(\Lambda_m^{\nu+1}(\Gamma^m) + \Gamma^m)/2$, respectively. In the stopping condition (4), we choose a small parameter $\varepsilon > 0$. In the following numerical computations, we took $\varepsilon = 10^{-15}$.

5.2 Numerical examples

In the following examples, several numerical computations of the evolution of N -sided polygons will be shown. The numerical solutions were computed until the time T_* with the uniform time increment $\tau = T_*/\bar{m}$, where \bar{m} is the maximum time step. The figures are depicted every M -th time step. The problems except Example 7 have the CAS property with μ_{CAS} , and the numerical solution keeps this property with the error $\Delta = \max_{0 \leq m < \bar{m}} |\mu_{\text{CAS}} - \mu_{\text{CAS}}^m|$, where $\mu_{\text{CAS}}^m = (|\Omega^{m+1}| - |\Omega^m|)/\tau$ is the m -th discrete area speed. The problem in Example 7 has CLS property with μ_{CLS} , and the numerical solution keeps this property with the error $\Delta = \max_{0 \leq m < \bar{m}} |\mu_{\text{CLS}} - \mu_{\text{CLS}}^m|$, where $\mu_{\text{CLS}}^m = (|\Gamma^{m+1}| - |\Gamma^m|)/\tau$ is the m -th discrete length speed. The following two tables indicate the data N , T_* , τ , M and Δ in each example.

	Ex.1: Figure 2			Ex.2: Figure 3	
	(left)	(middle)	(right)	(left)	(right)
N	5	7	22	7	
T_*	0.2801	0.3136	0.335	1.55	1.55
τ	10^{-6}			10^{-4}	10^{-7}
M	2801	3136	3350	775	775000
Δ	5.04×10^{-10}	7.62×10^{-10}	1.56×10^{-9}	2.87×10^{-11}	2.96×10^{-7}

Table 1: Numerical parameters and Δ for Examples 1 and 2.

	Ex.3: Figure 4		Ex.5: Figure 6	Ex.6: Figure 7		Ex.7: Figure 8
		(upper)	(lower)	(upper)	(lower)	
N	9	12	12	32		18
T_*	7.56	19.4	20	10	3.65	0.27
τ	10^{-5}		10^{-4}	10^{-4}		10^{-4}
M	37800	97000	10000	5000	1825	27
Δ	1.51×10^{-9}	1.07×10^{-9}	2.81×10^{-7}	4.26×10^{-9}	1.42×10^{-10}	5.11×10^{-11}

Table 2: Numerical parameters and Δ for Examples 4–7.

5.2.1 Example 1 — polygonal curvature flow

Figure 2 indicates the evolution of solution polygons to Problem 3.2, starting from the initial polygon being the outermost N -sided polygon which is a combination of an upper half of a regular $2(N-2)$ -polygon and a triangle. Each solution polygon evolves from outside to inside and has the CAS property with $\mu_{\text{CAS}} = -2 \sum_{j=1}^N \tan(\varphi_j/2)$. The numerical solutions keep the CAS property very accurately as shown in Table 1.

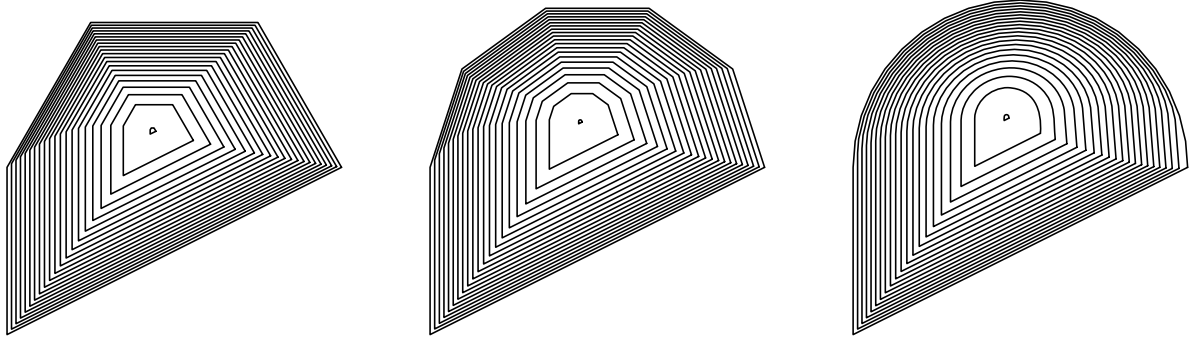


Figure 2: Evolution by polygonal curvature flow.

5.2.2 Example 2 — backward polygonal curvature flow

Problem 3.2 can be computed backward in time. Figure 3 (left) indicates the evolution of solution polygons to the backward polygonal curvature flow $V_j(t) = \kappa_j(t)$ ($j = 1, 2, \dots, 7$). The initial polygon is the innermost 7-sided polygon and the solution polygons evolve from inside to outside. The above process can be followed by our second order scheme accurately.

We note that the backward curvature flow for smooth curves is ill-posed since it becomes a backward parabolic problem. Actually, even in the case of 7-sided polygon's motion, it is hard to compute the backward polygonal curvature flow by using the Euler scheme (Problem 4.6). Figure 3 (right) indicates an easy breakdown of the Euler scheme

in spite of using a smaller τ than the one in the second order scheme.

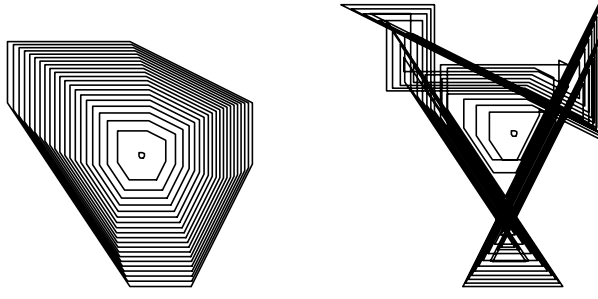


Figure 3: Simulations of the backward polygonal curvature flow by the second order scheme (left) and by the Euler method (right).

5.2.3 Example 3 — area-preserving polygonal curvature flow

Figure 4 (middle–upper/lower) shows two examples of polygonal motions according to Problem 3.3. The initial polygons are given as Figure 4 (left–upper/lower). Figure 4 (right–upper/lower) shows the final polygon and the initial polygon (dotted curve). The solution has CAS property with $\mu_{\text{CAS}} = 0$.

In both upper and lower examples, there exist stationary solutions as shown in Figure 5 (middle/right). The polygon starting from a symmetric initial shape approaches to one of the stationary solutions and stays there for a while. However, since the stationary solution has a saddle-point instability, after a while, the polygon is drifted away from the stationary solution along the unstable manifold and loses its symmetry.

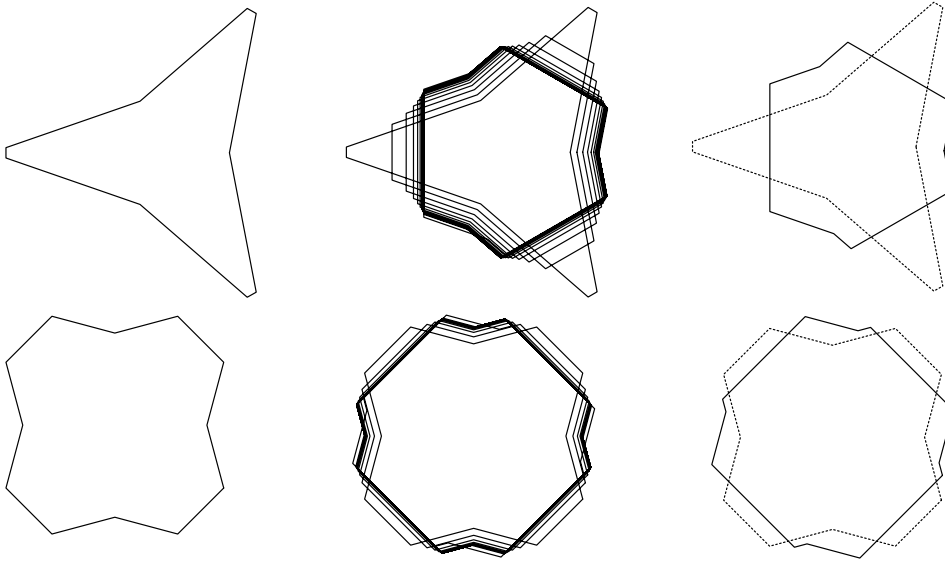


Figure 4: Evolutions by the area-preserving polygonal curvature flow.

5.2.4 Example 4 — stationary solutions

A polygon which has a constant polygonal curvature (i.e. $\kappa_1 = \dots = \kappa_N$) is a stationary solution of Problem 3.3. Obviously, regular polygons are stationary solutions. Besides the regular polygons, we have infinite many stationary solutions. For instance, an n -fold star shaped polygon is a stationary solution as well as the 6-fold star (Figure 5 (left)), and an n -fold non-sharp star shaped polygon is also a stationary solution as well as the 3-fold/4-fold non-sharp stars in Figure 5 (middle/right). For the n -fold non-sharp star polygon, there are two kinds of outer angles $\varphi_0 < 0$ and $\varphi_1 > 0$ and two kinds of edge lengths $d_1 < d_2$ with the corresponding polygonal curvatures: $\kappa_1 = (\tan(\varphi_0/2) + \tan(\varphi_1/2))/d_1$ and $\kappa_2 = 2 \tan(\varphi_1/2)/d_2$. We have constant polygonal curvature polygon if $d_1/d_2 = (\tan(\varphi_0/2) + \tan(\varphi_1/2))/(2 \tan(\varphi_1/2))$. The polygon in Figure 5 (middle/right) belongs to the same equivalence class of Figure 4 (upper/lower).

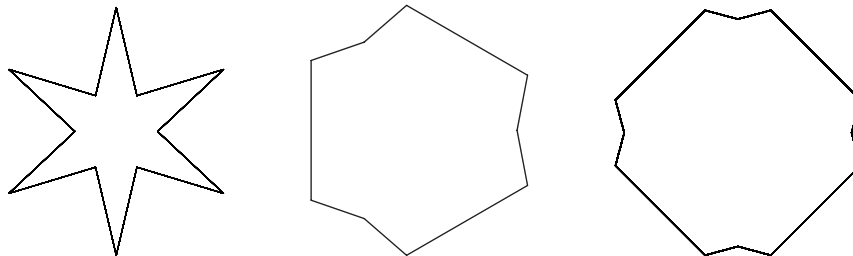


Figure 5: Stationary solutions of Problem 3.3.

5.2.5 Example 5 — polygonal advected flow with constant area speed

Figure 6 (middle) shows an example of polygonal motions according to Problem 3.4 with $\mathbf{u}(\mathbf{x}) = \mathbf{x}/(2\pi|\mathbf{x}|^2)$ which is a divergence-free vector field defined on $\mathbb{R}^2 \setminus \{\mathbf{0}\}$. The initial polygons are given as Figure 6 (left) whose center is the origin. Figure 6 (right) shows the final polygon and the initial polygon (dotted curve). The problem has the CAS property with $\mu_{\text{CAS}} = 1$. The numerical solution keeps the CAS property very accurately as shown in Table 2.

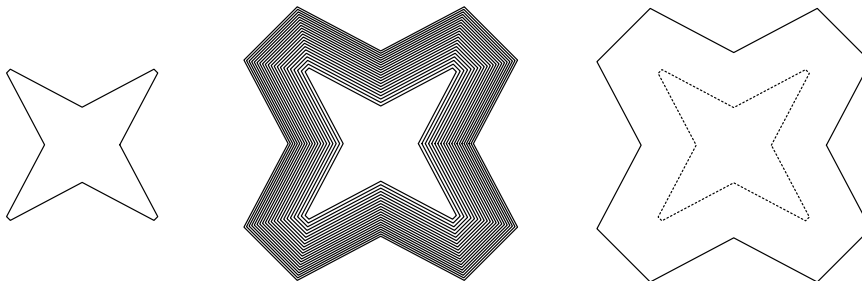


Figure 6: Evolution by polygonal advected flow with constant area speed.

5.2.6 Example 6 — area-preserving polygonal advected-curvature flow

Figure 7 (middle-upper/lower) shows two examples of polygonal motions according to combination of Problem 3.3 and Problem 3.4, i.e.,

$$V_j = \langle \kappa(\cdot, t) \rangle - \kappa_j(t) + \langle \mathbf{u} \rangle_j \cdot \mathbf{n}_j \quad (j = 1, \dots, N).$$

The divergence-free vector field is given by $\mathbf{u}(\mathbf{x}) = x_1 x_2 (-x_1, x_2)$ (upper) and $\mathbf{u}(\mathbf{x}) = (-x_1, x_2)$ (lower), respectively. The common initial polygon is given as Figure 7 (left-upper/lower), where the center is the origin the vertices are on the ellipse with ratio 3:1. Figure 7 (right-upper/lower) shows the final polygon and the initial polygon (dotted curve). The both problems have CAS property with $\mu_{\text{CAS}} = 0$ (area preserving), and the numerical solutions preserve their areas very accurately as shown in Table 2.

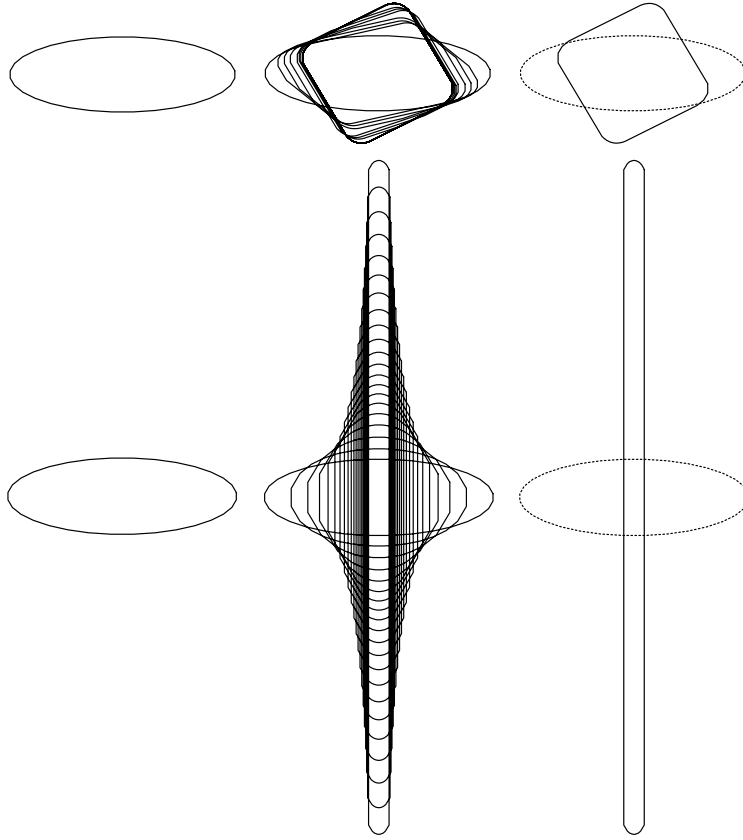


Figure 7: Evolution by area-preserving polygonal advected-curvature flow.

5.2.7 Example 7 — length-preserving polygonal curvature flow

Figure 8 (middle) shows the evolution of solution polygons to length-preserving polygonal curvature flow (4.17) given in Section 4.4. The initial polygon is the 18-sided polygon in Figure 8 (left). Figure 8 (right) indicates the final polygon and the initial polygon

(dotted curve). At the time close to T_* , the length of an edge (pointed by the arrow) tends to zero, and the computation stops. The length-preserving property ($\mu_{\text{CLS}} = 0$) is numerically realized with high accuracy as shown in Table 2.

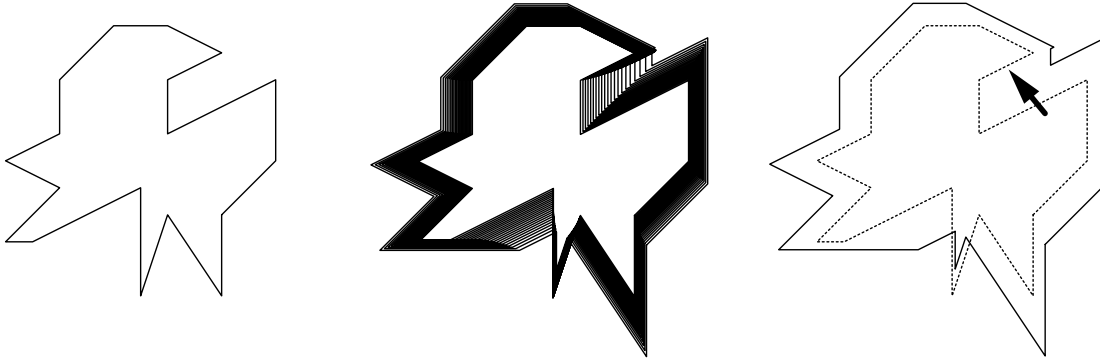


Figure 8: Evolution by the length-preserving polygonal curvature flow.

References

- [1] B. Andrews, *Singularities in crystalline curvature flows*, Asian J. Math. **6** (2002) 101–122.
- [2] S. Angenent and M. E. Gurtin, *Multiphase thermomechanics with interfacial structure, 2. Evolution of an isothermal interface*, Arch. Rational Mech. Anal. **108** (1989) 323–391.
- [3] M. Gage, *On an area-preserving evolution equation for plane curves*, D.M. DeTurck (Ed.), Nonlinear Problems in Geometry, Contemp. Math. **51** (1986) 51–62.
- [4] Y. Giga, *Surface evolution equations, A level set approach*, Monographs in Mathematics, 99. Birkhauser Verlag, Basel, (2006).
- [5] M.-H. Giga and Y. Giga, *Crystalline and level set flow – convergence of a crystalline algorithm for a general anisotropic curvature flow in the plane*, Free boundary problems: theory and applications, I (Chiba, 1999), GAKUTO Internat. Ser. Math. Sci. Appl., Gakkōtoshō, Tokyo **13** (2000) 64–79.
- [6] P. M. Girão, *Convergence of a crystalline algorithm for the motion of a simple closed convex curve by weighted curvature*, SIAM J. Numer. Anal. **32** (1995) 886–899.
- [7] P. M. Girão and R. V. Kohn, *Convergence of a crystalline algorithm for the heat equation in one dimension and for the motion of a graph by weighted curvature*, Numer. Math. **67** (1994) 41–70.

- [8] K. Ishii and H. M. Soner , *Regularity and convergence of crystalline motion*, SIAM J. Math. Anal. **30** (1999) 19–37.
- [9] T. Ishiwata , T. K. Ushijima , H. Yagisita and S. Yazaki, *Two examples of nonconvex self-similar solution curves for a crystalline curvature flow*, Proc. Japan Academy **80**, Ser. A, No. 8 (2004), 151–154.
- [10] T. Ishiwata and S. Yazaki, *On the blow-up rate for fast blow-up solutions arising in an anisotropic crystalline motion*, J. Comp. App. Math. **159** (2003), 55–64.
- [11] J. E. Taylor, *Motion of curves by crystalline curvature, including triple junctions and boundary points*, Diff. Geom.: partial diff. eqs. on manifolds (Los Angeles, CA, 1990), Proc. Sympos. Pure Math., **54** (1993), Part I, 417–438, AMS, Providencd, RI.
- [12] T. K. Ushijima and S. Yazaki, *Convergence of a crystalline algorithm for the motion of a closed convex curve by a power of curvature $V = K^\alpha$* , SIAM J. Numer. Anal. **37** (2000) 500–522.
- [13] T. K. Ushijima and S. Yazaki, *Convergence of a crystalline approximation for an area-preserving motion*, Journal of Computational and Applied Mathematics **166** (2004), 427–452.
- [14] S. Yazaki, *Asymptotic behavior of solutions to an expanding motion by a negative power of crystalline curvature*, Adv. Math. Sci. Appl. **12** (2002), 227–243.
- [15] S. Yazaki, *On an area-preserving crystalline motion*, Calc. Var. **14** (2002), 85–105.
- [16] S. Yazaki, *Motion of nonadmissible convex polygons by crystalline curvature*, Publications of Research Institute for Mathematical Sciences **43** (2007), 155–170.
- [17] S. Yazaki, *Asymptotic behavior of solutions to an area-preserving motion by crystalline curvature*, Kybernetika **43** (2007), 903–912.